

# Standard Fluorescent Imaging of Live Cells is Highly Genotoxic

Jing Ge,<sup>1</sup> David K. Wood,<sup>2</sup> David M. Weingeist,<sup>1</sup> Somsak Prasongtanakij,<sup>3</sup> Panida Navasumrit,<sup>3</sup> Mathuros Ruchirawat,<sup>3</sup> Bevin P. Engelward<sup>1\*</sup>

<sup>1</sup>Department of Biological Engineering, Massachusetts Institute of Technology, Cambridge, Massachusetts 02139

<sup>2</sup>Harvard-MIT Division of Health Sciences and Technology, Massachusetts Institute of Technology, Cambridge, Massachusetts 02139

<sup>3</sup>Environmental Toxicology Program, Chulabhorn Graduate Institute, Bangkok, Thailand

Received 11 December 2012; Revision Received 1 March 2013; Accepted 9 March 2013

Grant sponsor: NIH/NIEHS; Grant numbers: Primary support by 5-U01-ES016045; Partial support from P30-ES002109; 1-R21-ES019498; R43-ES021116-01; NIEHS Training Grant in Environmental Toxicology number T32-ES007020

\*Correspondence to: Bevin P. Engelward, Department of Biological Engineering, Massachusetts Institute of Technology, 77 Massachusetts Avenue, Cambridge, MA 02139, USA

Email: bevin@mit.edu

Published online 6 May 2013 in Wiley Online Library (wileyonlinelibrary.com)

DOI: 10.1002/cyto.a.22291

© 2013 International Society for Advancement of Cytometry

## • Abstract

Fluorescence microscopy is commonly used for imaging live mammalian cells. Here, we describe studies aimed at revealing the potential genotoxic effects of standard fluorescence microscopy. To assess DNA damage, a high throughput platform for single cell gel electrophoresis is used (e.g., the CometChip). Light emitted by three standard filters was studied: (a) violet light [340–380 nm], used to excite DAPI and other blue fluorophores, (b) blue light [460–500 nm] commonly used to image green fluorescent protein (GFP) and Calcein AM, and (c) green light [528–553 nm], useful for imaging red fluorophores. Results show that exposure of samples to light during imaging is indeed genotoxic even when the selected wavelengths are outside the range known to induce significant damage levels. Shorter excitation wavelengths and longer irradiation times lead to higher levels of DNA damage. We have also measured DNA damage in cells expressing enhanced GFP or stained with Calcein AM, a widely used green fluorophore. Data show that Calcein AM leads to a synergistic increase in the levels of DNA damage and that even cells that are not being directly imaged sustain significant DNA damage from exposure to indirect light. The nature of light-induced DNA damage during imaging was assessed using the Fpg glycosylase, an enzyme that enables quantification of oxidative DNA damage. Oxidative damage was evident in cells exposed to violet light. Furthermore, the Fpg glycosylase revealed the presence of oxidative DNA damage in blue-light exposed cells for which DNA damage was not detected using standard analysis conditions. Taken together, the results of these studies call attention to the potential confounding effects of DNA damage induced by standard imaging conditions, and identify wavelength, exposure time, and fluorophore as parameters that can be modulated to reduce light-induced DNA damage. © 2013 International Society for Advancement of Cytometry

## • Key terms

fluorescence microscopy; live cell imaging; genotoxicity; comet assay; light exposure; formamidopyrimidine-DNA glycosylase (Fpg)

**FLUORESCENCE** microscopy is a powerful approach for studying a broad range of cellular and tissue responses. Furthermore, by specifically labeling molecules in cells and by taking images in real time, fluorescence microscopy is a powerful tool that provides detailed and instant visualization of cells. Snapshots allow researchers to obtain static optical information of tissue, cells, or subcellular compartments. On the other hand, fluorescence microscopy can also be performed in a dynamic mode by selecting fluorescent molecules that allow for sequential image collection and analysis over a span of time (e.g., using propidium iodide (PI) in the real-time for dynamic cell viability assays, or tagging membrane molecules to monitor cell division). However, a major barrier to fluorescence microscopy is the fact that light exposure can have an impact on cellular responses. While it is known that UV light can induce substantial cellular DNA damage by causing pyrimidine dimers (1,2), little has been done to explore the possible genotoxic effects of light and fluorophores used in fluorescence microscopy.

The wavelengths of light used in fluorescence microscopy generally range from 350 nm to 800 nm. Light exposure can lead to different types of cellular DNA damage, varied by the wavelength it possesses (1,2). Short wavelength light in the range of UVC (100–280 nm) and UVB (290–320 nm) can initiate direct excitation of DNA and generate photoproducts such as cyclobutane pyrimidine dimers and pyrimidine (6-4) pyrimidone (3,4). On the other hand, longer wavelength UVA (420–400 nm) and blue light are genotoxic due to their ability to produce reactive oxygen species that can give rise to base damage (i.e., 8-hydroxyguanine) and direct strand breaks (5–8). Although the mechanisms of light-induced genotoxicity can be different, depending on the wavelength it possesses, the mutagenicity and carcinogenicity of light irradiation are well-established (9–15).

In addition to directly induced DNA damage, fluorophores used to make cells visible are themselves photosensitizers, which can lead to the formation of short-lived radicals that react with cellular constituents after excitation by light (16). Common fluorescent molecules used in microscopy include PI, green fluorescent protein (GFP), Calcein AM, 4',6-diamidino-2-phenylindole (DAPI), and Hoechst 33342, which are used in wide applications of monitoring cell viability, growth, migration, differentiation, and many other intracellular reactions (17–24). The cytotoxic or phototoxic effects of some fluorescent dyes used during microscopy have been previously reported (18,25–28); however, little is known about their effect on cellular genome.

To study potential lesions induced during fluorescence microscopy, we took advantage of the single cell electrophoresis assay, also known as the comet assay (29,30). Briefly, to perform the comet assay, cells are embedded in agarose, the membranes are lysed, and the cell is subjected to electrophoresis. When the DNA in the nucleoids is subjected to electrophoresis, fragmented or nicked loops of damaged DNA migrate more readily than the supercoiled nuclear matrix. By measuring the amount of migrated “tail” DNA relative to the supercoiled “head,” the extent of DNA damage can be quantified (29–32). By altering the pH, the assay can be tuned to detect single strand breaks, alkali sensitive sites, and abasic sites (alkaline conditions) or to detect double strand breaks (neutral conditions) (31,32). A modified version of the assay can also be performed to detect specific base lesions. This is achieved by inclusion of purified lesion-specific enzymes that converts undetectable base lesion into detectable strand breaks (31,33–35).

Recently, microfabrication techniques were used to create a platform for high throughput analysis of DNA damage using the comet assay (36). Here we have assessed the genotoxic effects induced by standard fluorescence imaging of live cells using a high throughput comet assay platform engineered by Wood et al. This device, called the CometChip, spatially registers cells in arrays of microwells so that multiple exposure conditions can be evaluated on single agarose gel (36). Here, we describe optimization of a 96-well version of the CometChip wherein each well of the 96-well plate (named as a “macrowell”) has at its base hundreds of microwells (with dimension in micrometers). In addition, we show that specific

classes of DNA damage can be monitored on this platform using the modified comet assay, using the repair endonuclease formamidopyrimidine-DNA glycosylase (Fpg) to reveal oxidative DNA modifications (this is an approach that has previously been shown to be effective for the traditional comet assay; see (33,34)). The major goal of this work is to evaluate the potential genotoxic impact of standard fluorescent imaging of live cells, and to identify conditions that minimize genotoxicity.

## MATERIALS AND METHODS

### Cell Culture

TK6 human lymphoblasts were cultured in suspension in 1× Roswell Park Memorial Institute (RPMI) medium 1640 with L-glutamine supplemented with 10% horse serum (Invitrogen, Grand Island, NY). Chinese hamster ovarian AA8 and U2OS cells were cultured in 1× Dulbecco's Modified Eagle Medium (DMEM) with L-glutamine supplemented with 10% FBS (Invitrogen). Regular and IRES-GFP U2OS cells were obtained from Dr. Scott Floyd (MIT, Cambridge, MA). All cell culture media were supplemented with 100 units/mL penicillin–streptomycin (Invitrogen, Grand Island, NY) and cultivation was performed at 37°C in an atmosphere of 5% CO<sub>2</sub>. Live cells in Figure 1D were stained with CellTracker (Invitrogen).

### CometChip Fabrication

The CometChip Polydimethylsiloxane (PDMS) molds were fabricated using the protocols described by Wood et al. (36). Molds with 40- $\mu$ m diameter microposts were allowed to float on molten 1% normal melting point agarose (Invitrogen) on top of a sheet of GelBond film (Lonza, Hopkinton, MA) (Fig. 1A). After the mold was removed, the agarose gel with microwells that were attached to GelBond film was placed on a glass plate and a bottomless 96-well plate (Greiner BioOne, Hopkinton, MA) was pressed onto the gel and clamped to create the multiwell version of the comet platform, the CometChip. A 100  $\mu$ L of cells ( $10^5$ – $10^6$  cells/mL) were pipetted into each of the 96-well and captured in microwells by gravity. The bottomless 96-well plate was then removed and the gel was covered with 1% low melting point agarose (Fig. 1B).

### Light Exposure

After encapsulation in agarose, cells were either first stained with Calcein AM (Invitrogen) or directly irradiated by light under  $\times 10$  objective lens of the Nikon 80i upright microscope coupled with an automatic scanning stage. The Nikon 80i uses a 120W Mercury Arc Lamp (Exfo, Quebec, Canada) as light source. Light of different wavelengths were obtained by using three different filters: UV-2E/C, FITC HYQ, and G-2E/C (Figs. 2A and 2B, Table 1). The intensities of the each light were measured for three times using Auto-Ranging Light Meter (Amprobe, Everett, WA), averaged and listed in Table 1, the error is calculated as the standard deviation of the three measurements. Each multiwell was scanned at same speed for different amount of time to allow for different exposure/imaging times. Wells that were adjacent to scanned/irradiated wells receive indirect exposure (Fig. 3A). After exposure, sam-

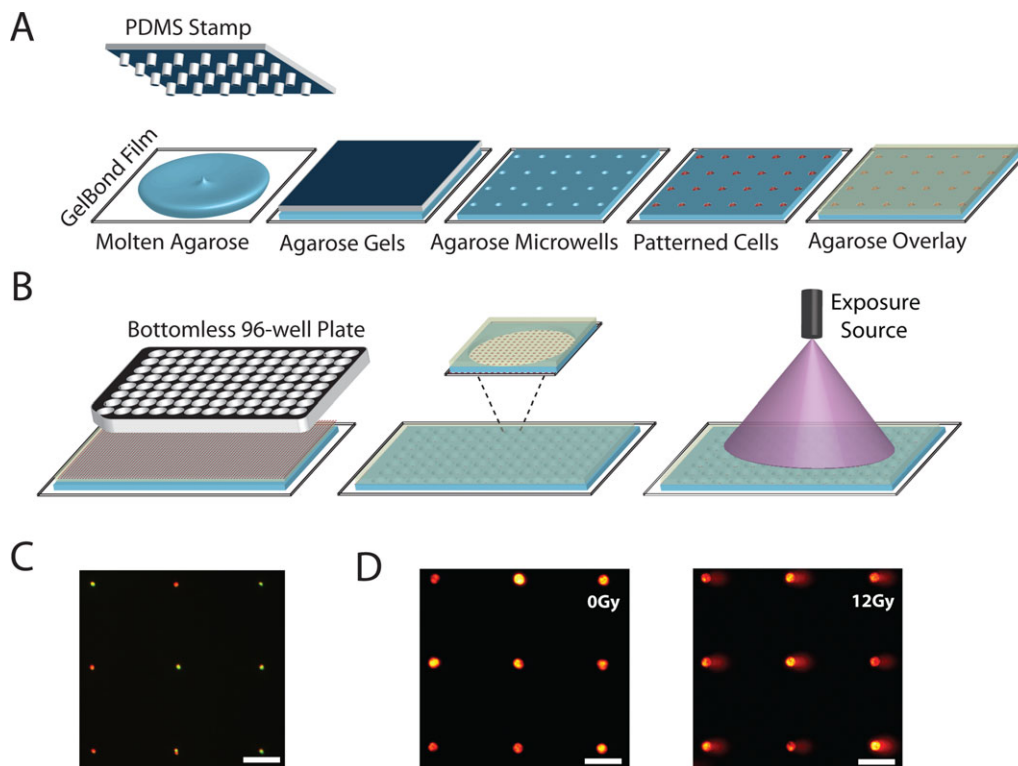


**Figure 1.** High throughput comet analysis platform. **A:** A microfabricated PDMS stamp with microposts is placed onto molten agarose. After the agarose gels, the stamp is removed and cells are loaded into the microwells by gravity. An agarose overlay encloses cells. **B:** To create the CometChip, a bottomless 96-well plate is pressed on agarose gel with embedded cell array that is placed on a glass substrate to create the macrowell platform (each well of the 96-well plate is considered to be a single macrowell). Each macrowell has within it ~300 microwells loaded with cells. **C:** Single cell loading in microwells. Two populations of cells stained red and green were loaded concurrently. **D:** Arrayed non-irradiated (left) and 12-Gy irradiated (right) microwell comets observed under 10 $\times$  objective lens. Monochrome images were collected from microscope camera and colored with Red Hot lookup Table using Image J. Horizontal scale bars are 100  $\mu$ m.

ples were immediately removed from the scanning stage and placed into standard lysis solution at 4 $^{\circ}$ C.

### Comet Assay

After overnight lysis, CometChips were placed into an electrophoresis chamber filled with alkaline unwinding buffer (0.3 M NaOH and 1 mM Na<sub>2</sub>EDTA) for 40 min at 4 $^{\circ}$ C. Electrophoresis was performed at the same temperature with the same buffer for 30 min at 1 V/cm and a current of 300 mA. The chips were then neutralized twice for 15 min in fresh buffer (0.4 M Tris-HCl at pH 7.5) and at 4 $^{\circ}$ C.

### Fluorescence Imaging and Comet Analysis

After neutralization, the CometChips were stained with SYBR Gold (Invitrogen) according to the manufacturer's instructions. Images were captured using the same microscope and analyzed using the Guicometanalyzer, a custom software written in MatLab (The Mathworks, Beltsville, MD) by Wood et al. (36) as previously described (code available upon request).

### Fapy Glycosylase

After overnight lysis and before comet assay was performed, CometChips were removed from lysis buffer and

washed three times for 15 min in enzyme reaction buffer (40 mM HEPES, 0.1 M KCl, 0.5 mM EDTA, 0.2 mg/mL Bis(trimethylsilyl)acetamide (BSA) at room temperature. Buffer was made fresh and adjusted to pH 8.0 with KOH. Fapy glycosylase stocks (New England Biolab, Ipswich, MA) were diluted in enzyme reaction buffer by 10,000 times. Samples were placed in square petri dishes with approximately 10–15 mL of enzyme solution and transferred into a 37 $^{\circ}$ C incubator. After 40 min of enzyme digestion, samples were washed and stored in fresh cold buffer (no enzyme) at 4 $^{\circ}$ C until normal unwinding.

## RESULTS

### Analysis of DNA Damage Using CometChip

Conditions developed by Wood et al. (36) were optimized to create a 96-well platform. Specifically, a PDMS stamp with arrayed microposts is used to cast agarose gel with arrayed microwells. Each microwell is approximately 40  $\mu$ m in diameter, a diameter that works effectively to capture the cell types used in our experiments (data not shown). After allowing cells to settle into the microwells by gravity, arrayed cells we captured using an agarose overlay (Fig. 1A). The macrowell compartments of the CometChip were created by pressing a bottomless 96-well plate onto the agarose

gel. Each macrowell can then be exposed to different exposure source at different dose to allow for high throughput analysis of multiple experiments on the same agarose gel at the same time (Fig. 1B). Figure 1C shows single cell loading using cell populations that were stained green or red to demonstrate single cell capture. The efficacy of the CometChip for detection of DNA damage caused by ionizing

radiation (IR) is shown in Figure 1D. The length of the tail corresponds to the extent of DNA damage.

### DNA Damage in Cells Exposed to Light During Imaging

In standard fluorescent imaging of live cells, both the light source and fluorescent labels are potential sources of genotoxicity. Here, we have to decouple the source of damage by first studying the genotoxic effects of light source alone. Unlabeled TK6 cells encapsulated in CometChips were irradiated by light from fluorescent microscope under procedures identical to live imaging (described in Materials and Methods). Light with three non-overlapping wavelength brackets (340–380 nm [violet], 460–500 nm [blue], and 528–553 nm [green]) were studied by using the bandpass excitation filters indicated in Figures 2A and 2B, Table 1. The center wavelengths (CWL) of these lights are 360 nm (violet), 480 nm (blue), and 540 nm (green), respectively. The intensities of these lights were measured to be 0.11 W/m<sup>2</sup> (violet), 6.52 W/m<sup>2</sup> (blue), and 89.89 W/m<sup>2</sup> (green), respectively (listed in Table 1.). We focused on these wavelengths because of their extensive use in live cell imaging. The shortest wavelength, violet light, which was obtained using a UV-2E/C filter, is normally used to excite fluorophores that emits blue fluorescence such as DAPI and Hoechst 33342. Exposure to violet light for 15 min causes the most DNA damage (Fig. 2C). Blue and green light, which are commonly used to excite fluorescent molecules that give a green and red fluorescent image respectively, produce low to minimal damage (Fig. 2C). It is noteworthy that although the longer wavelength lights (blue and green) possess intensities that are significantly higher than the violet light, they appear to be much less genotoxic. Thus, light-induced DNA damage is highly wavelength-dependent and nominally intensity-dependent.

In studies of cellular responses over a long span of time (28), the same population of cells must be repeatedly imaged. A caveat is that repetitive and extended periods of light and long exposure should not exert stress that would disrupt cellular responses. Here, we tested a range of imaging times for their genotoxic potential. Cells exposed under violet light (360

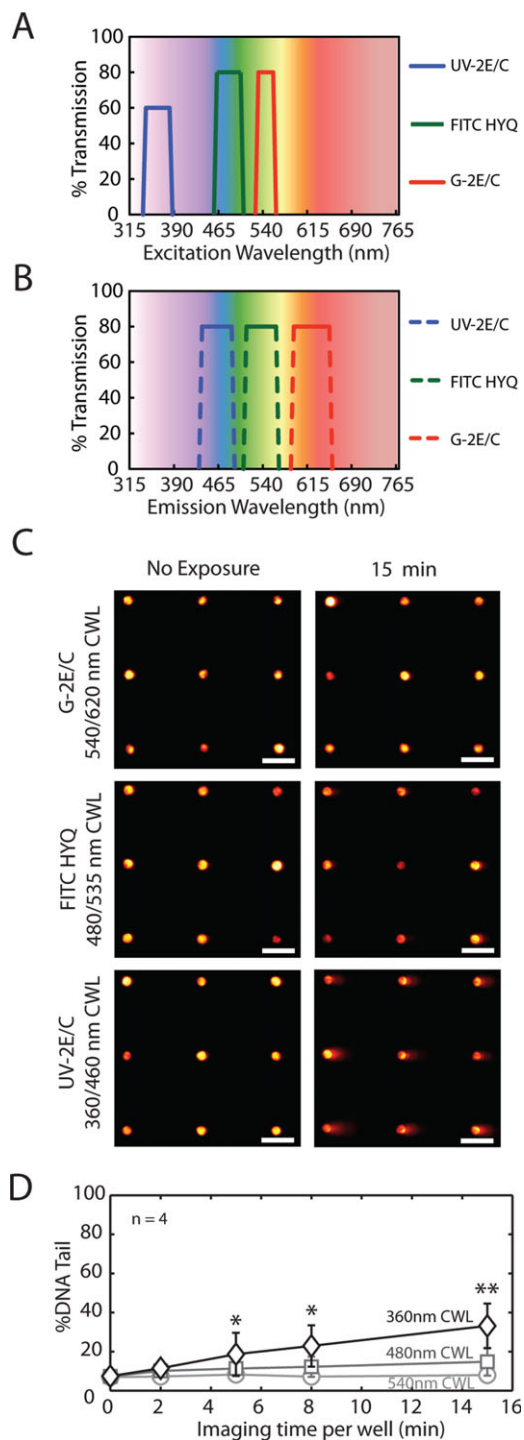


**Figure 2.** Fluorescence microscopy excitation light-induced damage. Nikon 80i microscope fluorescent filter (A) excitation and (B) emission spectrum (data compiled from manufacturer, Nikon). Filter names are according to manufacturer's nomenclature. All filters are band pass filters with wavelength brackets plotted and center wavelength (CWL) listed in Table 1. C: Arrayed microwell comets with varying exposure times to the specified wavelengths. Monochrome images were collected from microscope camera and colored with Red Hot lookup Table using Image J. Horizontal scale bars are 100  $\mu$ m. D: Comparison of light-induced damage under varying imaging/exposure times using TK6 human lymphoblasts. Each data point is the average of four independent experiments, where the median % DNA Tail of 100 individual comets was used to represent the extent of DNA damage. Error bars represent standard error of the four repeats. Symbols indicate a significant difference compared to non-exposed TK6 (Imaging time per well = 0 min) according to Student's *T*-test: \* $P < 0.05$ , \*\* $P < 0.005$ .



**Table 1.** Microscope filter specifications and excitation light intensities.

FILTER NAME	EXCITATION FILTER WAVELENGTH <sup>A</sup>	EXCITATION LIGHT INTENSITY <sup>B</sup>	BARRIER FILTER WAVELENGTH <sup>C</sup>	COMMON FLUOROPHORES IMAGED
UV-2E/C	340–380 nm (bandpass, 360 CWL)	0.11 ± 0.00 W/m <sup>2</sup>	435–485 nm (bandpass, 460 CWL)	DAPI
FITX HYQ	460–500 nm (bandpass, 480 CWL)	6.52 ± 0.04 W/m <sup>2</sup>	510–560 nm (bandpass, 535 CWL)	GFP, FITC, Calcein AM
G-2E/C	528–553 nm (bandpass, 540 CWL)	89.89 ± 1.27 W/m <sup>2</sup>	590–650 nm (bandpass, 620 CWL)	EtBr, PI

<sup>a,c</sup> Data compiled from manufacturer (Nikon)

<sup>b</sup> Data measured using Light Meter (Amprobe), error reflects standard deviation of three measurements

nm CWL) for longer than 5 min had significantly higher damage level than other samples, and the amount of DNA damage increases linearly with exposure time (Fig. 2D). Exposing wells for 5 min and 8 min resulted in 19% and 23% damage respectively, with  $P < 0.05$  (Student's *T*-test) compared to unexposed samples. When the imaging time reached 15 min per well, the damage level rose significantly, to about 33% ( $P < 0.005$ ). Samples exposed to blue light (480 nm CWL), on the other hand, only showed significant damage at the longest time point tested (15 min;  $P < 0.05$ ). Green light (540 nm CWL) did not show any detectable impact on cellular DNA (Fig. 2D). A comparison between different wavelengths was also performed in which we found that 360 nm CWL violet light induced significantly higher levels of DNA damage at 8 min ( $P < 0.05$ ) and 15 min ( $P < 0.005$ ) compared to green light (540 nm CWL). These results show that shorter wavelength light is more damaging than the longer wavelengths (at least for the wavelengths that we tested), and that DNA damage increases when exposure time is increased. The results shown here are a useful criterion to guide wavelength selection for experiments where cells will be exposed to light for extended periods of time.

### Impact of Direct Light and Indirect Light on DNA Damage in Cells Labeled with Calcein-AM and GFP

As fluorescent imaging cannot be performed without labeling cells with a fluorophore, we next explored the combinatorial effect of light exposure and the presence of fluorophores on genotoxicity. There are two commonly used approaches for rendering cells fluorescent: (1) expression of a fluorescent protein; or (2) staining using fluorophores. To explore these conditions, we used U2OS cells that express GFPs, wild type U2OS cells stained with Calcein AM, and non-fluorescent wild type U2OS. We set to evaluate and compare GFP and Calcein AM because: (a) they are mostly commonly practiced in live cell imaging (especially GFP as it is the first identified fluorescent protein) and (b) they have very similar excitation and emission spectrum (GFP is excited at 490 nm and emits maximally at 509 nm, Calcein AM excitation peaks at 494 nm and emits maximally at 517 nm) which is compatible with the FITC HYQ filter (Figs. 2A and 2B). As a result, we hypothesize that if GFP and Calcein AM exerts different genotoxic impacts, such difference can be attributed to the fluorophore itself.

While direct exposure is a concern, indirect exposure might also be problematic. When specimens are placed in close proximity to allow for fast and high throughput imaging (i.e., in 96-well plates), cells that are adjacent to directly imaged wells may be exposed to indirect light (Fig. 3A). Although the intensity of indirect light will be lower, fluorophores in cells may still be excited and light exposure may still lead to considerable genotoxicity. We therefore examine the impact of indirect light using the 96-well platform provided by the CometChip. When the well in center was directly imaged or exposed by light from the microscope lamp, surrounding wells were exposed to a reduced level of indirect light (Fig. 3A).

While blue light (480 nm CWL) was not potentially genotoxic to unstained cells (Figs. 2D and 3B), Calcein AM caused a synergistic increase in the levels of DNA damage (Fig. 3B). Damage levels exceeded 80% with as little as 2 min of exposure (Fig. 3B), which is the maximum level of damage that can be detected using the comet assay. The upper limits of detection are consistent with the plateau in damage levels that is observed in Figure 3B. Interestingly, cells that express GFP did not show a significant amount of damage under any time point tested. The discrepancy between Figure 3B and Figure 2D at the longest imaging time (15min) using blue light can be attributed to difference in sensitivity and damage response in different cell lines (TK6 vs. U2OS cells). Remarkably, the impact of Calcein AM was also observed in cells exposed only to indirect light. Although the damage levels are lower than under direct exposure, damage levels in neighboring wells rose significantly, from ~20% to ~40% when imaging time was increased from 2 to 15 min (Fig. 3C). These results clearly demonstrate that labeling cells with Calcein AM dramatically sensitizes cells to light-induced genotoxicity, whereas GFP labeling does not significantly impact the levels of DNA damage.

To put the observed damage levels into perspective, we have compared the impact of light exposure to that of IR. Figure 3D shows that Calcein-AM stained cells exposed only to indirect light attain damage level equivalent to 4–6 Gy IR. Since the damage levels in directly exposed cells had reached saturation, one cannot infer a corresponding radiation dose, but clearly the impact would be far greater. Looking at just the effect of indirect light, the equivalent dose of 2–4 Gy  $\gamma$ -IR is highly genotoxic. Indeed, just 2 Gy of IR is enough to increase the mutation frequency by one or more orders of magnitude

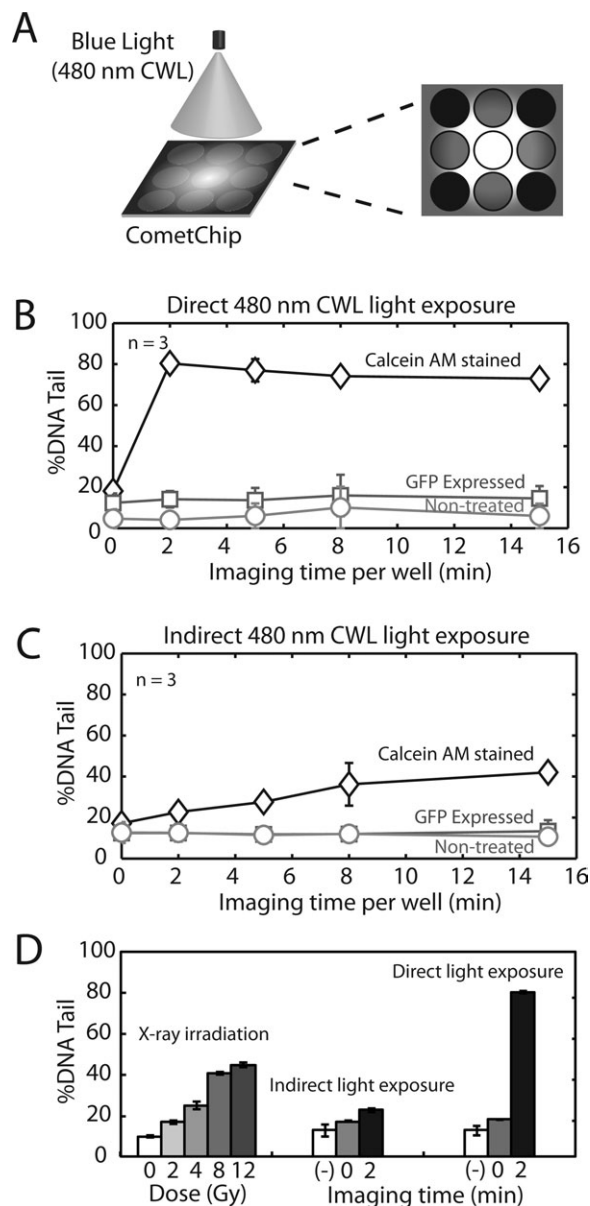


**Figure 3.** Direct and indirect light-induced damage in fluorescent cells. **A:** Diagram indicating indirect light exposure in neighboring wells when imaging the center well. **B,C:** DNA damage levels in U2OS cells exposed to direct and indirect blue light (480 nm CWL) from microscope. Data for control cells, cells expressing GFP, and Calcein AM-stained U2OS cells are shown. **D:** Comparison of damage levels from X-ray irradiation and fluorescent imaging using Calcein AM. (-) represent wild type U2OS cells un-stained with Calcein AM. Data and error bars represent averages and standard errors of three independent experiments.

(37,38). Furthermore, DNA damage responses have been observed in vivo with as little as 1 cGy of radiation exposure (39–41), which raises the possibility that wells even more distant than those next to the exposed well may show a significant DNA damage response. Taken together, the magnitude of the genotoxic impact of light-induced DNA damage in Calcein AM stained cells is likely to induce significant changes in DNA

sequence, and to trigger DNA damage response pathways (42,43), even in cells that are only indirectly exposed to light.

### Glycosylase-Mediated Conversion of Damaged Bases into Single Strand Breaks for Detection Using the CometChip

While light is well known for its ability to induce pyrimidine dimers (3,4), light can also induce genotoxic reactive oxygen species (6–8). Indeed, 300–500 nm light predominantly induces oxidative DNA modifications, rather than dimers (7). Exposing DNA to reactive oxygen species leads to over a dozen types of damaged bases. Some of the more common lesions are repaired by the base excision repair (BER) pathway. In response to oxidative damage, the Fapy glycosylase (Fpg) initiates BER by recognizing damaged bases (including 8-oxoguanine and formamidopyrimidines), removing the damaged base, and cleaving the backbone. Both violet light (360 nm CWL) and blue light (480 nm CWL) therefore have the potential to induce oxidative DNA damage. Therefore, to determine whether the lesions induced are due to oxidative stress, we used a modified version of the comet assay that exploits purified Fpg (33,34). To perform this assay, cells are embedded in the microarray, exposed to light, and the cells are lysed. Following lysis, the gels are washed and then incubated with buffer containing Fpg. Incubation with the glycosylase enables conversion of undetectable base damage into detectable single strand breaks. As a positive control, cells were exposed to  $H_2O_2$ . The addition of Fpg resulted in a two-fold increase in the levels of DNA damage in  $H_2O_2$  treated cells ( $P < 0.01$ , Student's *T*-test; Fig. 4A), as expected. The addition of Fpg to the comets of undamaged cells resulted in what appears to be a slight increase in damage, though the result was not statistically significant. Taken together, these data are consistent with Fpg converting undetectable  $H_2O_2$ -induced base lesions into detectable single strand breaks, thus demonstrating that Fpg can be used to reveal the presence of oxidatively damaged bases.

To learn whether exposure to light during microscopy can lead to a significant increase in oxidative damage, we exposed TK6 lymphoblasts to 360 nm CWL [violet], 480 nm CWL [blue], and 540 nm CWL [green] light. With only 5 min exposure time, there was not a significant increase in DNA damage in the TK6 cells exposed to any of the wavelengths (Fig. 4B), which is consistent with the results shown in Figure 2, with the exception that violet light induced a small amount of DNA damage in the U2OS cells (a difference that is consistent with variation among cell types). Although there was no observable increase in DNA damage in the TK6 cells with light alone, we hypothesized that undetectable damaged bases may nevertheless be present. To reveal the potential presence of damaged bases, we therefore treated the lysed comets with Fpg. Light-induced DNA damage is indeed sensitive to Fpg cleavage, as can be seen by the increase in damage level from ~12% to ~40% in cells exposed to violet (360 nm CWL) and blue (480 nm CWL) light (note that in Fig. 4B, the order of the wavelengths is reverse to emphasize the increase in damage that coincides with the shorter wavelengths). Importantly, in

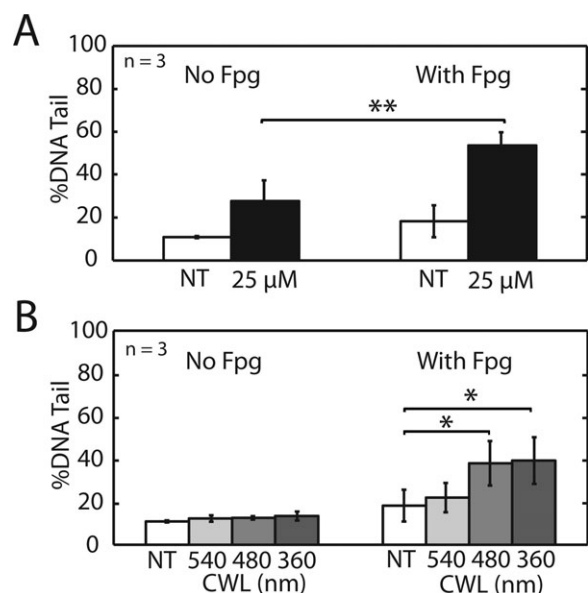


**Figure 4.** Oxidative DNA base lesions revealed by the Fpg glycosylase. TK6 cells in the CometChip were exposed to (A) 25  $\mu$ M H<sub>2</sub>O<sub>2</sub> or (B) 5 min light of different CWLs, lysed and incubated with Fpg glycosylase to reveal oxidative damage. Data and error bars represent averages and standard errors of three independent experiments. Symbols indicate significance according to Student's *T*-test: \**P* < 0.05, \*\**P* < 0.01.

cells exposed to blue light (480 nm CWL), no damage was detected using standard comet assay conditions, and the presence of damage was revealed when sites with DNA damage were cleaved by Fpg. These data demonstrate that light exposure during fluorescent live cell imaging induces oxidative DNA damage. It is noteworthy that the shorter wavelength light induced oxidative damage, whereas the longer wavelength green light (540 nm CWL) did not cause a detectable increase in DNA damage levels. Having revealed the presence of oxidative DNA damage even at relatively short exposure times (and without the presence of Calcein AM), this study calls attention to the possibility that DNA damage and DNA damage responses may impact the results of studies using live-cell imaging.

## DISCUSSION

Given the rapid rise in fluorescence imaging for broad applications, we have investigated the potential biological impact of the imaging process itself, which has the potential to be an important confounding factor in experiments. To explore the inherent genotoxicity of standard fluorescence microscopy, we used a high throughput DNA damage platform developed in our laboratory (36). Results here show that both light during imaging and fluorophores are potentially genotoxic, and delineate variables that can be modulated to suppress genotoxicity, including wavelength, duration, proximity, and the nature of the fluorophore.

To learn about the impact of wavelength, light emitted from three standardly used filters for fluorescence microscopy were investigated: violet light (360 nm CWL, standardly used

for excitation of DAPI), blue light (480 nm CWL, used for visualizing green fluorescence), and green light (540 nm CWL, used for visualizing red fluorescence). To query genotoxicity, we used the comet assay wherein the extent of DNA damage is reflected in the extent to which DNA migrates away from the nucleus when electrophoresed. Using the alkaline comet assay, which detects single strand breaks, abasic sites, and alkali sensitive sites, very little DNA damage was induced by either blue or green light. In contrast, just 5 min of exposure to violet light causes a significant increase in DNA damage. To put the damage levels into perspective, we treated cells with IR, which is known to be mutagenic, cytotoxic, and potentially carcinogenic. The levels of damage induced by 5 min of exposure to violet light are comparable to the damage levels observed in cells exposed to  $\sim$ 2 Gy of  $\gamma$ -IR. Research shows that 1–2 Gy IR causes more than 1,000 base damage, about 40 double strand breaks and 1,000 single strand breaks (44), a level of damage sufficient to trigger cell cycle arrest and cytotoxicity (45,46). More subtle effects, such as the triggering of damage response pathways, are expected to occur at much lower doses (39–41). Thus, there are likely to be very significant damage response pathways even with quite short exposure times.

UV light have wavelengths ranging from 100 to 400 nm, and thus includes the shortest wavelength studied here, violet light (360 nm CWL). UV dimers are formed most readily by light in the UVC range (100–290 nm) and to some extent in the UVB range (290–320) (7), both of which are below the shortest wavelengths that are standardly used in fluorescence microscopy. Consequently, it is a commonly held belief that DNA damage is avoided during fluorescence imaging. What is less well appreciated is the potential for longer wavelengths to induce oxidative DNA damage, which includes single strand breaks and a broad range of damaged DNA bases (5–8). Here, we directly addressed the potency of commonly used excitation wavelengths to specifically induce oxidative damage to DNA. To accomplish this objective, we took advantage of the Fpg glycosylase, a bifunctional DNA glycosylase that recognizes oxidized bases, removes the damage, and cleaves the DNA backbone. Using this enzyme, it is possible to convert base lesions, which cannot be detected using the alkaline comet assay, to single strand breaks, which can be detected. Data show that violet light, found to be most damaging using the standard alkaline comet assay, is indeed associated with a significant induction of oxidative damage. Interestingly, although blue light appeared to be only mildly damaging using the standard assay conditions, Fpg revealed that there are actually high levels of oxidative damage. The detailed mechanisms involved in the generation of oxidative DNA modifications remain to be established; however there is a strong belief that natural endogenous and exogenous photosensitizers play an important role (7). They could react with DNA directly via a type I reaction or via singlet oxygen as the result of type II photosensitization mechanism (7,47). Taken together, our data demonstrate that commonly used conditions for fluorescence microscopy can induce oxidative DNA adducts, through reactions of photosensitizers in cells. Some of the most abundant lesions generated from light exposure,

such as 8-oxo-7,8-dihydro-2'-deoxyadenosine (48) (also a substrate of Fpg protein), can give rise to considerable deleterious impact on cells due to their high miscoding and mutagenic properties (13,49).

Fluorescence microscopy requires the presence of fluorophores, some of which are known to be photosensitizers. We therefore explored the DNA damaging potential of two very commonly used fluorophores: Calcein AM and GFP. Calcein AM is useful for a broad range of applications, including viability assays (50–52), and studies of cell migration, chemotaxis, cell adhesion, and membrane permeability (53–57). Calcein AM and its derivatives have been widely used in part because of their apparently low cytotoxicity. In addition to Calcein AM, we also studied the impact of GFP expression, which is often used for long-term cell labeling. Both of these green fluorophores are visualized during microscopy using blue light (480 nm CWL) as the excitation wavelength. Unexpectedly, cells stained with Calcein AM are dramatically sensitive to blue light-induced DNA damage, compared to control cells or cells expressing GFP. This was somewhat unexpected, since Calcein AM is a cytoplasmic stain that does not bind to or intercalate into DNA. One possible explanation for the synergistic effect of light exposure in combination with the presence of Calcein AM is that excited Calcein AM may act as a strong photosensitizer. When exposed to light, photosensitizers are known to be able to trigger the formation of singlet oxygen and/or oxygenated products within a cell (58). Regardless of the underlying mechanism, these data demonstrate the genotoxic potential of fluorophores during imaging.

In many cases, the exposure time for one sample is relatively short, thus minimizing the genotoxic effects of imaging. However, using common high throughput conditions that employ 96-well plates, it is important to consider the possibility that cells in wells that are not being directly imaged might be nevertheless be damaged by indirect exposure. Although there was not a detectable increase in DNA damage in control cells exposed to indirect light, cells that were stained with Calcein AM had high levels of DNA damage. Importantly, even in the control cells that appeared to be undamaged, it remains likely that there is nevertheless a significant amount of oxidative damage that is not detected under the conditions used in this experiment. High throughput screens are now being used to identify novel cancer chemotherapeutics, many of which are DNA damaging agents. These results call attention to the importance of careful consideration of the potential confounding effects of imaging itself.

Today's imaging technologies are opening doors to unprecedented opportunities for screening and monitoring cell behavior. Little attention, however, has been given to the potential importance of genotoxicity that might be induced concomitantly during the imaging process. For many experiments, DNA damage could be confounding. Even under conditions when light-induced DNA damage is relatively mild, DNA damage response pathways could be triggered, which have broad effects, including modulation of DNA repair and triggering cell cycle arrest. The results of these studies call

attention to the importance of wavelength, exposure time, sample position, and fluorophores as important variables to consider during live-cell imaging.

#### ACKNOWLEDGMENTS

Equipment for data analysis was provided by the Center for Environmental Health Sciences P30-ES002109. We thank Scott Floyd for the U2OS cell lines.

#### LITERATURE CITED

1. Tyrrell RM, Keyse SM. New trends in photobiology. The interaction of UVA radiation with cultured cells. *J Photochem Photobiol B Biol* 1990;4:349–361.
2. Moan J, Peak MJ. Effects of UV radiation of cells. *J Photochem Photobiol B Biol* 1989;4:21–34.
3. Besaratinia A, Yoon J-I, Schroeder C, Bradforth SE, Cockburn M, Pfeifer GP. Wavelength dependence of ultraviolet radiation-induced DNA damage as determined by laser irradiation suggests that cyclobutane pyrimidine dimers are the principal DNA lesions produced by terrestrial sunlight. *FASEB J* 2011;25:3079–3091.
4. Pfeifer GP, You Y-H, Besaratinia A. Mutations induced by ultraviolet light. *Mutat Res* 2005;571:19–31.
5. Peak JG, Peak MJ. Comparison of initial yields of DNA-to-protein crosslinks and single-strand breaks induced in cultured human cells by far- and near-ultraviolet light, blue light and X-rays. *Mutat Res* 1991;246:187–191.
6. Hattori-Nakakuki Y, Nishigori C, Okamoto K, Imamura S, Hiai H, Toyokuni S. Formation of 8-hydroxy-2'-deoxyguanosine in epidermis of hairless mice exposed to near-UV. *Biochem Biophys Res Commun* 1994;201:1132–1139.
7. Kielbassa C, Roza L, Epe B. Wavelength dependence of oxidative DNA damage induced by UV and visible light. *Carcinogenesis* 1997;18:811–816.
8. Pflaum M, Will O, Epe B. Determination of steady-state levels of oxidative DNA base modifications in mammalian cells by means of repair endonucleases. *Carcinogenesis* 1997;18:2225–2231.
9. Ananthaswamy HN, Pierceall WE. Molecular mechanisms of ultraviolet radiation carcinogenesis. *Photochem Photobiol* 1990;52:1119–1136.
10. Brash DE, Rudolph JA, Simon JA, Lin A, McKenna GJ, Baden HP, Halperin AJ, Pontén J. A role for sunlight in skin cancer: UV-induced p53 mutations in squamous cell carcinoma. *Proc Natl Acad Sci USA* 1991;88:10124–10128.
11. Kress S, Sutter C, Strickland PT, Mukhtar H, Schweizer J, Schwarz M. Carcinogen-specific mutational pattern in the p53 gene in ultraviolet B radiation-induced squamous cell carcinomas of mouse skin. *Cancer Res* 1992;52:6400–6403.
12. Sage E. Distribution and repair of photolesions in DNA: Genetic consequences and the role of sequence context. *Photochem Photobiol* 1993;57:163–174.
13. Wood ML, Dizdaroglu M, Gajewski E, Essigmann JM. Mechanistic studies of ionizing radiation and oxidative mutagenesis: Genetic effects of a single 8-hydroxyguanine (7-hydro-8-oxoguanine) residue inserted at a unique site in a viral genome. *Biochemistry* 1990;29:7024–7032.
14. Shibutani S, Takeshita M, Grollman AP. Insertion of specific bases during DNA synthesis past the oxidation-damaged base 8-oxodG. *Nature* 1991;349:431–434.
15. Gushima M, Hirahashi M, Matsumoto T, Fujita K, Fujisawa R, Mizumoto K, Nakabeppu Y, Iida M, Yao T, Tsuneyoshi M. Altered expression of MUTYH and an increase in 8-hydroxydeoxyguanosine are early events in ulcerative colitis-associated carcinogenesis. *J Pathol* 2009;219:77–86.
16. Epe B, Pflaum M, Boiteux S. DNA damage induced by photosensitizers in cellular and cell-free systems. *Mutat Res* 1993;299:135–145.
17. Zhao H, Oczos J, Janowski P, Trembecka D, Dobrucki J, Darzynkiewicz Z, Wlodkowic D. Rationale for the real-time and dynamic cell death assays using propidium iodide. *Cytometry A* 2010;77A:399–405.
18. Shi L, Günther S, Hübschmann T, Wick LY, Harms H, Müller S. Limits of propidium iodide as a cell viability indicator for environmental bacteria. *Cytometry A* 2007;71A:592–598.
19. Martin RM, Leonhardt H, Cardoso MC. DNA labeling in living cells. *Cytometry A* 2005;67A:45–52.
20. Kondo N, Miyauchi K, Matsuda Z. Monitoring viral-mediated membrane fusion using fluorescent reporter methods. *Curr Protoc Cell Biol* 2011;Chapter 26:Unit 26.9.
21. Mahmoud L, Al-Saif M, Amer HM, Sheikh M, Almajhdi FN, Khabar KSA. Green fluorescent protein reporter system with transcriptional sequence heterogeneity for monitoring the interferon response. *J Virol* 2011;85:9268–9275.
22. Uggeri J, Gatti R, Belletti S, Scandroglio R, Corradini R, Rotoli BM, Orlandini G. Calcein-AM is a detector of intracellular oxidative activity. *Histochem Cell Biol* 2004;122:499–505.
23. Chen Z, Zhang Z, Gu Y, Bai C. Impaired migration and cell volume regulation in aquaporin 5-deficient SPC-A1 cells. *Respir Physiol Neurobiol* 2011;176:110–117.
24. Sørensen G, Pedersen DV, Nørgaard AK, Sørensen KB, Nygaard SD. Microbial growth studies in biodiesel blends. *Bioresour Technol* 2011;102:5259–5264.
25. Spötl L, Sarti A, Dierich MP, Möst J. Cell membrane labeling with fluorescent dyes for the demonstration of cytokine-induced fusion between monocytes and tumor cells. *Cytometry* 1995;21:160–169.
26. Samlowski WE, Robertson BA, Draper BK, Prystas E, McGregor JR. Effects of supravital fluorochromes used to analyze the in vivo homing of murine lymphocytes on cellular function. *J Immunol Methods* 1991;144:101–115.



27. Oh DJ, Lee GM, Francis K, Palsson BO. Phototoxicity of the fluorescent membrane dyes PKH2 and PKH26 on the human hematopoietic KG1a progenitor cell line. *Cytometry* 1999;36:312–318.
28. Purschke M, Rubio N, Held KD, Redmond RW. Phototoxicity of Hoechst 33342 in time-lapse fluorescence microscopy. *Photochem Photobiol Sci* 2010;9:1634–1639.
29. Singh NP, McCoy MT, Tice RR, Schneider EL. A simple technique for quantitation of low levels of DNA damage in individual cells. *Exp Cell Res* 1988;175:184–191.
30. Ostling O, Johanson KJ. Microelectrophoretic study of radiation-induced DNA damages in individual mammalian cells. *Biochem Biophys Res Commun* 1984;123:291–298.
31. Collins AR. The comet assay for DNA damage and repair: Principles, applications, and limitations. *Mol Biotechnol* 2004;26:249–261.
32. Olive PL, Banáth JP. The comet assay: A method to measure DNA damage in individual cells. *Nat Protoc* 2006;1:23–29.
33. Georgakilas AG, Holt SM, Hair JM, Loftin CW. Measurement of oxidatively-induced clustered DNA lesions using a novel adaptation of single cell gel electrophoresis (comet assay). *Curr Protoc Cell Biol* 2010;Chapter 6:Unit 6.11.
34. Fortini P, Raspaglio G, Falchi M, Dogliotti E. Analysis of DNA alkylation damage and repair in mammalian cells by the comet assay. *Mutagenesis* 1996;11:169–175.
35. Collins AR, Dusinská M, Horská A. Detection of alkylation damage in human lymphocyte DNA with the comet assay. *Acta Biochim Pol* 2001;48:611–614.
36. Wood DK, Weingeist DM, Bhatia SN, Engelward BP. Single cell trapping and DNA damage analysis using microwell arrays. *Proc Natl Acad Sci USA* 2010;107:10008–10013.
37. Tindall KR, Stein J, Hutchinson F. Changes in DNA base sequence induced by gamma-ray mutagenesis of lambda phage and prophage. *Genetics* 1988;118:551–560.
38. Yang N, Galick H, Wallace SS. Attempted base excision repair of ionizing radiation damage in human lymphoblastoid cells produces lethal and mutagenic double strand breaks. *DNA Repair (Amst)* 2004;3:1323–1334.
39. Amundson SA, Do KT, Shahab S, Bittner M, Meltzer P, Trent J, Fornace AJ. Identification of potential mRNA biomarkers in peripheral blood lymphocytes for human exposure to ionizing radiation. *Radiat Res* 2000;154:342–346.
40. Fujimori A, Okayasu R, Ishihara H, Yoshida S, Eguchi-Kasai K, Nojima K, Ebisawa S, Takahashi S. Extremely low dose ionizing radiation up-regulates CXC chemokines in normal human fibroblasts. *Cancer Res* 2005;65:10159–10163.
41. Gruel G, Voisin P, Vaurijoux A, Roch-Lefevre S, Grégoire E, Maltere P, Petat C, Gidrol X, Voisin P, Roy L. Broad modulation of gene expression in CD4+ lymphocyte subpopulations in response to low doses of ionizing radiation. *Radiat Res* 2008;170:335–344.
42. Jeggo P, Löbrich M. Radiation-induced DNA damage responses. *Radiat Prot Dosimetry* 2006;122:124–127.
43. Little JB. Radiation carcinogenesis. *Carcinogenesis* 2000;21:397–404.
44. Hall EJ, Giaccia AJ. *Radiobiology for the Radiologist*. Philadelphia: LWW; 2012.1 p.
45. Landsverk KS, Lyng H, Stokke T. The response of malignant B lymphocytes to ionizing radiation: Cell cycle arrest, apoptosis and protection against the cytotoxic effects of the mitotic inhibitor nocodazole. *Radiat Res* 2004;162:405–415.
46. Puck TT, Marcus PI. Action of X-rays on mammalian cells. *J Exp Med* 1956;103:653–666.
47. Pouget JP, Douki T, Richard MJ, Cadet J. DNA damage induced in cells by gamma and UVA radiation as measured by HPLC/GC-MS and HPLC-EC and Comet assay. *Chem Res Toxicol* 2000;13:541–549.
48. Cadet J, Douki T, Ravanat J-L. Oxidatively generated damage to the guanine moiety of DNA: Mechanistic aspects and formation in cells. *Acc Chem Res* 2008;41:1075–1083.
49. Moriya M, Takeshita M, Johnson F, Peden K, Will S, Grollman AP. Targeted mutations induced by a single acetylaminofluorene DNA adduct in mammalian cells and bacteria. *Proc Natl Acad Sci USA* 1988;85:1586–1589.
50. Roden MM, Lee KH, Panelli MC, Marincola FM. A novel cytotoxicity assay using fluorescent labeling and quantitative fluorescent scanning technology. *J Immunol Methods* 1999;226:29–41.
51. Wang XM, Terasaki PI, Rankin GW, Chia D, Zhong HP, Hardy S. A new microcellular cytotoxicity test based on calcein AM release. *Hum Immunol* 1993;37:264–270.
52. Cortvrintd RG, Smitz JE. Fluorescent probes allow rapid and precise recording of follicle density and staging in human ovarian cortical biopsy samples. *Fertil Steril* 2001;75:588–593.
53. Rust WL, Huff JL, Plopper GE. Screening assay for promigratory/antimigratory compounds. *Anal Biochem* 2000;280:11–19.
54. Simpson MA, Reiland J, Burger SR, Furcht LT, Spicer AP, Oegema TR, McCarthy JB. Hyaluronan synthase elevation in metastatic prostate carcinoma cells correlates with hyaluronan surface retention, a prerequisite for rapid adhesion to bone marrow endothelial cells. *J Biol Chem* 2001;276:17949–17957.
55. Ko K, Arora P, Lee W, McCulloch C. Biochemical and functional characterization of intercellular adhesion and gap junctions in fibroblasts. *Am J Physiol Cell Physiol* 2000;279:C147–C157.
56. Zhang L, Rozek A, Hancock RE. Interaction of cationic antimicrobial peptides with model membranes. *J Biol Chem* 2001;276:35714–35722.
57. Gillissen T, Grasshoff C, Szinicz L. Mitochondrial permeability transition can be directly monitored in living neurons. *Biomed Pharmacother* 2002;56:186–193.
58. Smith KC. *The Science of Photobiology*. New York: Plenum Pub Corp; 1989.1 p.